ScienceVolks Open Access

SVOA MATERIALS SCIENCE & TECHNOLOGY

(ISSN: 2634-5331)

Research

https://sciencevolks.com/materials-science/

Volume 2 Issue 4

The Effect of Cooling Rate on the Microstructure of A356 Aluminium Alloy

Maftah H. Alkathafi[1*], Abdalfattah A. Khalil[2], Ayad O. Abdalla[3]

Affiliations:

[1]*Mechanical Engineering Department, Faculty of Engineering, Sirte University, Libya*

[2]*Materials Science Department, Faculty of Engineering, Omer Al-Mukhtar University, Libya.*

[3]*College of Mechanical Engineering Technology, Benghazi-Libya.*

***Corresponding author:** Maftah H. Alkathafi* *Mechanical Engineering Department, Faculty of Engineering, Sirte University, Libya*

Received: *December 10, 2020* ***Published:*** *December 31, 2020*

Abstract:

In this study a fast-cooling technology is employed for a cast iron mould to prepare cast A356 aluminium alloy by solidification of the molten metal. The cooling rate is achieved by pouring the molten alloy into a preheating permanent mould at different temperatures (25, 100, 200, 300 and 400^{0}C) for cast samples with 40 mm inside diameter and 200 mm height. The samples considered are analyzed by optical microscopy, scanning electron microscopy (SEM), and EDS X-ray analysis (EDS). The effects of cooling rate on the morphology of α – aluminum and eutectic silicon of A356 alloy have been studied. The results showed that the dendritic structure of α-phase was broken and converted into a somewhat globular grain structure and the coarse acicular eutectic silicon trend to be broken and converted into short sticks or small rounded in other cases.

Keywords: A356 Aluminum alloy, Grain refinement, Cooling rate, SEM, EDS, Microstructure.

1. Introduction

Aluminium alloys have attractive physical and mechanical properties. They are lightweight, low costs production, easy to machine and have good recycling possibilities up to 95 % [1]. Recently, it has been estimated that 20% of the total world-wide aluminum production is converted into cast components and about 70% of all aluminum castings are used in the transport industry, in particular in the automotive sector [2].

Cast aluminum alloy is one of the most well-developed aluminum alloys which is widely employed in industrial weight sensitive applications, such as aeronautics and space flight, because of its low density and excellent castability [3]. The effect of high cooling rates in producing fine structures results in development of high-strength cast alloys. The undercooling of a melt to a lower temperature increases the number of effective nuclei relative to the growth rate, the latter being restricted by the rate at which the latent heat of crystallization can be dissipated. The refining influence of an enhanced cooling rate applies both to primary grain size and substructure. Fast cooling during solidification is regarded as the most effective grain refinement approach for cast metals due to the large undercooling achieved, which promotes nucleation in the melt. It has been shown that the morphology and size of eutectic silicon are depended on cooling rate in the as-cast conditions [4-6]. The objective of the present study was to investigate the effect of cooling rate on α – aluminum and eutectic silicon morphology of A356 alloy that was performed on casting samples with various cooling rates.

2. Experimental Work

2.1 Materials

In this investigation a commercial Aluminium – Silicon based alloy, A356, was used with a chemical composition as provided by the supplier “ASTM” is shown in Table 1.

Table 1. Chemical composition(wt.%) of A356 "ASTM".

	Si	Fe	Cu	Mn	Mg	Zn	Ti	Other	Al
Min	6.5	-	-	-	0.20	-	-	-	
Max	**7.5**	**0.6**	**0.25**	**0.35**	**0.45**	**0.35**	**0.25**	**0.15**	**Balance**

This alloy was supplied from Aluminium Company of Egypt in the ingot form of A356-1, the delivered alloy of A356 was chemically analysed (actual analysis) with the help of optical immersion process and the result is shown in Table 2.

Table 2. Chemical composition(wt%) of the A356 alloy that applied in this study.

Si	Fe	Cu	Mn	Mg	Zn	Ti	Other	Al
7.36	**0.15**	**0.0462**	**0.00129**	**0.329**	**0.00229**	**0.136**	**0.012**	**Balance**

The Aluminium – Silicon phase diagram shows that the equilibrium eutectic constitution is about 12.6 wt.% silicon. Figure 1 shows that the aluminum-silicon eutectic can form as follows:

- Directly from the liquid in the case of a silicon concentration of 12.6%, for a eutectic aluminum-silicon alloy.
- In the presence of primary aluminum in the case of silicon contents less than 12.6%, for hypoeutectic aluminum-silicon alloys, and
- In the presence of primary silicon crystals in the case of silicon contents greater than 12.6%, for hypereutectic aluminum-silicon alloys.

The chosen aluminium alloy in this study consider as in a hypoeutectic Al-Si alloy. Its liquidus temperatures started at 614°C and solidification ended at 577°C (eutectic temperature). The microstructure comprises both primary FCC- aluminium solid solution containing 1.65wt% silicon and eutectic containing silicon enriched aluminium and pure silicon [7].

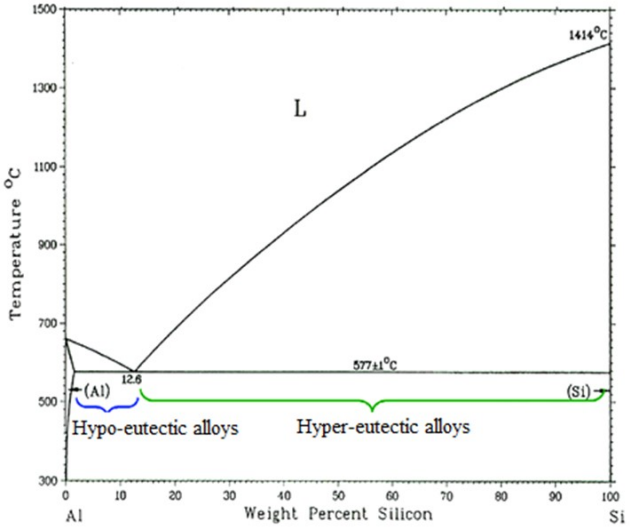

Figure 1. *Al-Si phase diagram showing hypo-and hyper-eutectic alloys.*

2.2 Cooling Rate Techniques

1500 g of A356 alloy was melted in a heat resistance furnace by using a steel crucible coated from inside with graphite. After complete melting of the alloy, the temperature of the molten metal was kept at a temperature of 740 °C± 10 °C, which is higher than its liquidus temperature by about 125 °C to allow the complete dissolution of the silicon particles. The used mould was preheated before pouring to study different conditions of solidified at different cooling rate. The pouring of melted alloy was carried out into a preheating permanent mould made of cast iron. The mould is kept at different temperatures (25, 100, 200, 300 and 400 ºC), the dimension of permanent mould was 40 mm inside diameter and 200 mm height for each step. Type K-Thermocouple (chromel–alumel) is accurate, inexpensive and has a wide temperature range, this type of thermocouple was used in measuring the temperature during melting and solidification. The thermocouple was calibrated before and after each series of melts.

2.3 The Microstructure Analysis

Metallographic samples were cut from the same position for all experiments at distance 15 mm from the bottom of casting as shown in Figure 2 and prepared according to used procedures developed for aluminum alloys. The investigated specimens were obtained under different solidification condition at different temperatures (25, 100, 200, 300 and 400 ºC). The samples for microstructure analysis were taken from each cast sample by sectioning the cylinders parallel to its longitudinal axis, three specimens for microstructure analysis were made from one section. The samples were cut and grinding using standard metallographic procedures. The grinding was done by using 240, 320, 400, and 600 grit papers. After grinding process, the samples were polished using 1 µm, and 0.05 µm Alumina suspension in water. A final polishing was performed using silica suspension. The samples were thoroughly cleaned after each step.

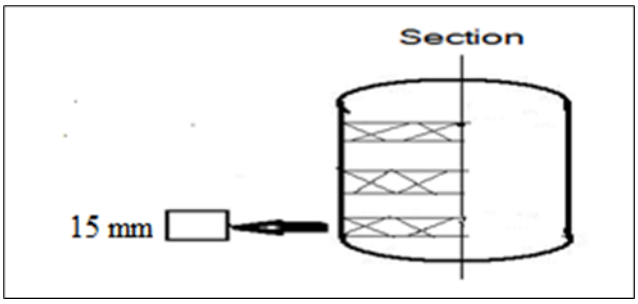

Figure 2. *location of specimens from bottom of cast cylinder of aluminum alloy A356.*

2.4 The Optical Microscopy and Quantitative Characterization

The samples that are used for characterization optical microscopy were etched using 0.5% HF solution to reveal the resulting microstructure [8]. Grain size, length, and width of both eutectic silicon and α - aluminum are measured by linear intercept method applied to the microstructure obtained from polarized light in optical microscope at 400X. Six digital micrographs are processed using image C- software. Average of ten readings is taken from the results.

2.5 The Scanning Electron Microscopic

The Scanning Electron Microscope (SEM) was used for the observation of the three-dimensional α-aluminum phase, eutectic Si morphology and analysis of composition of intermetallic phase of the specimens by deep-etched solution. Two deep etchants techniques were used in this study. Firstly, specimens were immersed in solution of 30 % NaOH in distilled water at temperature of 70 °C for certain time from 3 to 20 minutes [9]. Secondly, specimens were immersed in a solution of 15cm^{3}HCl, 10cm^{3}HF and 90cm^3 H_2O (distilled water) for a time from 15 to 20 minutes. Then, the specimens were immersed in water from 1 to 2 minutes, thereafter in alcohol for 3-5 minutes. Finally, the specimens were held in the dryer at temperature of 80 °C for about 60 minutes.[10].

3. Results and Discussion

3.1 The Microstructure of Base Alloy A356

An optical image of the base alloy-A356 after etching is shown in Figure 3(a), the microstructure shows the overall matrix and eutectic Si morphology, respectively. The microstructure of the as-cast aluminum alloys A356 is a fully dendritic structure of α solid solution and eutectic silicon. Furthermore, Figure 4(a) indicates a coarse acicular eutectic silicon dispersed among the fully developed dendritic primary α-aluminum "white" and eutectic silicon "dark gray". The average length of its primary dendritic arm was up to 1400µm, one branch of a primary α-aluminum was about 600 µm in length, as shown in Figure 4(a), which illustrated that the grain size was about a few millimeters as one grain usually contained several arms.

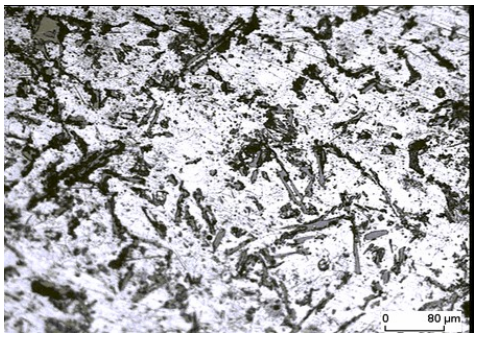

(a) Base alloy

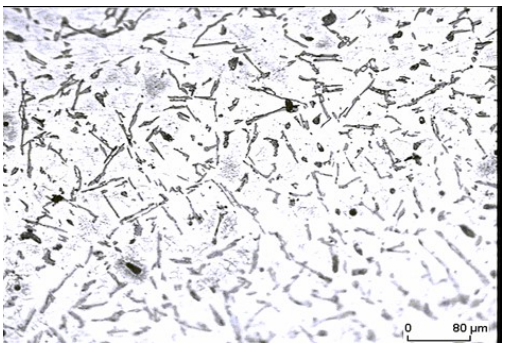

(d) At 200 °C

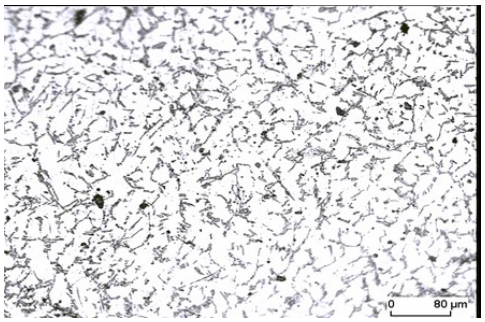

(b) At 25 °C

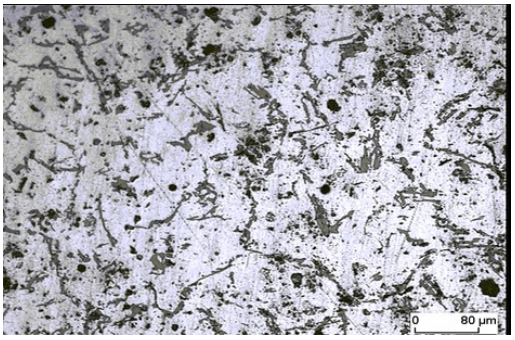

(e) At 300 °C

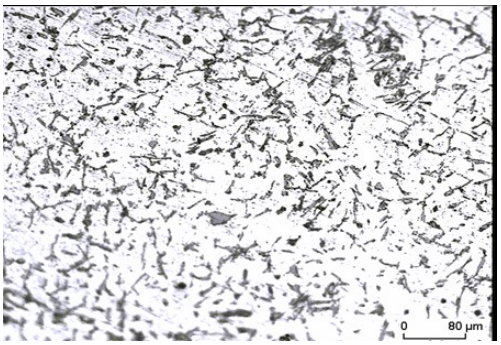

(c) At 100 °C

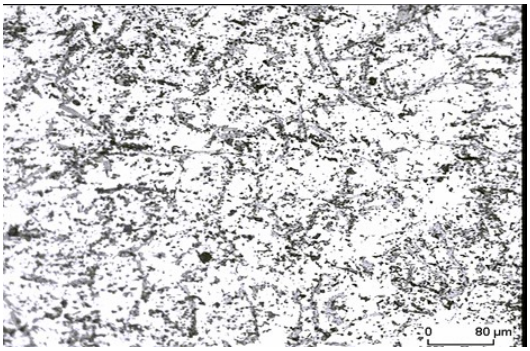

(f) At 400 °C

Figure. 3 *Optical micrograph of A356*

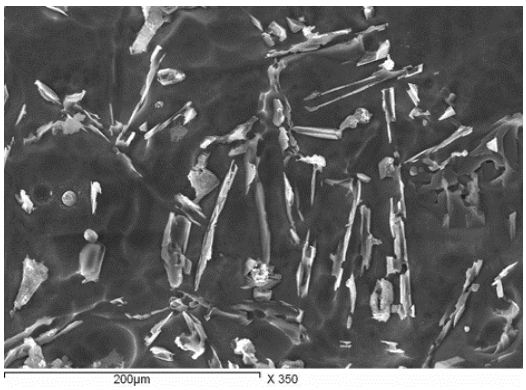

(a) Base alloy

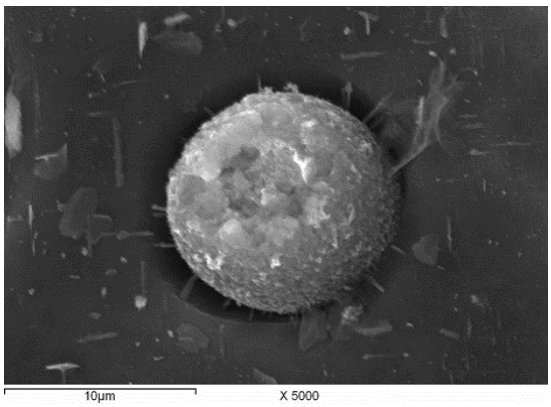

(b) Intermetallic phase

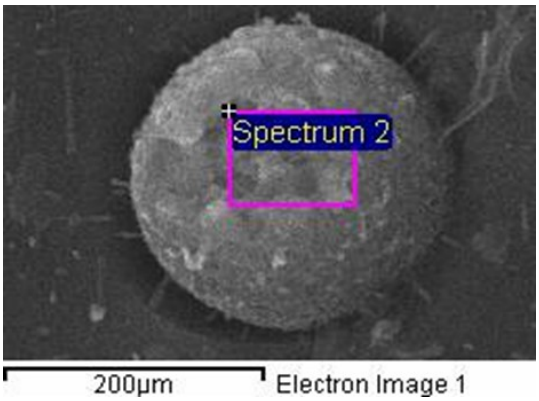

(c) Intermetallic phase

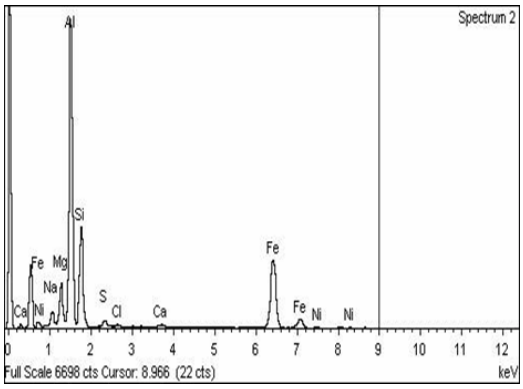

(d) EDS

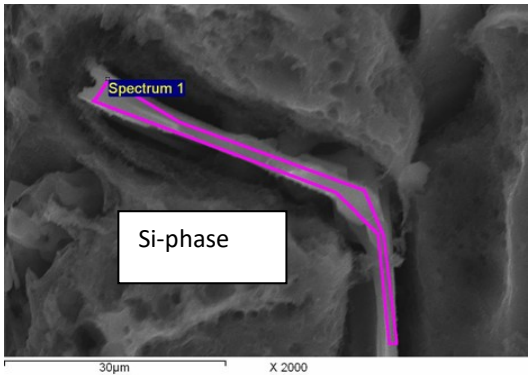

(e) Base alloy

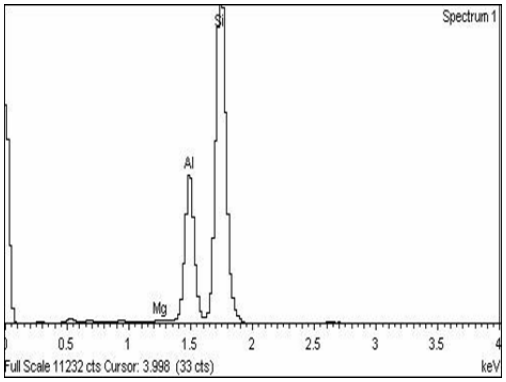

(f) EDS

Figure.4 : *SEM photographs of A356*

The microstructure of the hypoeutectic aluminum alloys (such as A356) usually consists of coarse dendritic α-Al solid solution and Al–Si eutectic, where Si usually observed as long plate or big spheres shape. Energy Dispersive X-ray Spectroscopy (EDS) was performed to investigate the nature and composition of samples which are characterized by SEM, as shown in Figure 4. It could be clearly seen that the microstructure of the investigated alloy is exhibited fully dendritic for each α- aluminum, coarse eutectic silicon and other intermetallic phase at a high magnification 350X. In addition, it can be seen that the small spherical particle of intermetallic phase is impeded inside the matrix. An EDS analysis presented in the Figure 4(b-d) were carried out to look into the nature and chemical composition of such small spherical particles shape, which were observed in the matrix. The EDS X-ray analysis verified that these particles that shown in the eutectic areas were mainly consists of inter-metallic phases of Al, Fe and Si. In the particular case of hypoeutectic A356 alloy, besides a usually coarse and dendritic α- Al solid solution and eutectic Si, the eutectic Si observed as large plate like morphology. The chemical composition of the inter-metallic phases, like "Chinese script" shaped could be described as α-$Al_{15}(Mn,Fe)_3Si_2$ and long sharp needles as β-Al_5FeSi, which precipitate in the interdendritic and intergranular regions. Puga et. al. [11] were also reported that the same interme-tallic phase in hypoeutectic $AlSi_9Cu_3$ alloy. Moreover, its highly detrimental effect on mechanical properties, this morphology could promote shrink-age porosity since the platelets restrict feeding by causing physical restrictions to the movement of compensatory feeding liquid, as reported by Liu et al [12].

Other researchers reported that the presence of intermetallic phases like the eutectic Al_2Cu, "Chinese script" shaped α-Al_{15} $(Mn, Fe)_3Si_2$ and long sharp needles of β-Al_5FeSi, which precipitate in the interdendritic and intergranular regions, and are strongly detrimental to the alloy mechanical and fatigue properties [11-13]. The EDS X-ray analysis of Figure 4(e) is showed in Figure 4(f), it is verified that the needle in the eutectic areas consisted mainly of silicon rather than intermetallic phases or inclusions. The needle-like compound contains the elements of Si, Al and Mg atoms, as illustrated in Figure 4(f), however, it consisted mainly of eutectic silicon and aluminum, respectively. As stated in the report [14], the needle particles that in im-peded in the α – aluminum is mainly consists of eutectic silicon. The eutectic silicon is formed between an aluminum solid solution containing just over 1% silicon and virtually pure silicon as the second phase. The eutectic composition has been a matter of debate, however, the recent experiments with high purity binary alloys has shown that the eutectic composition is Al–12.6 Si, with the transformation occurring at 577.6 °C. The slow solidification of a pure Al–Si alloy produces a very coarse microstructure in which the eutectic comprises large plates or needles of silicon in a continuous aluminum matrix, as shown in Figure 4(a,e) and Figure5. The eutectic itself is composed of individual cells within which the silicon particles appear to be interconnected [7].

3.2 The Effect of Cooling Rate on α-Phase

Figure 3(a-f) shows the comparison of the obtained microstructures. In the base specimen, the microstructure indicates a dendritic structure with average grain size of about a few millimeters. When the cooling rate technique is applied, the den-dritic structure of α-phase was broken up and converted into a somewhat globular grain structure. In the case of permanent mould casting, the rapid cooling is greatly refined the microstructure and hence the tensile strength is much improved. The eutectic may also be refined by the process known as modification. It is found that the better fine equiaxed globular grains has been observed in Figure 3(b) at the mould temperature of 25 ºC. Therefore, the optimum condition of preheating perma-nent mould was found at a temperature of 25 ºC. Furthermore, the average grain size for each investigated permanent mould temperature and different cooling rate were determined using linear intercept method (software); the results are shown in Table 3.

Table 3. Average grain size of α – aluminium

Mould temperature (ºC)	25	100	200	300	400
Average grain size (µm)	507	522	549	559	571

The decrease in grain size could be associated with decreasing in the mould temperature. This indicated that a grain refining effect could be achieved by increasing in the mould temperature. The grain size showed an inverse relationship to the number of solidified nuclei presented in the liquidus, which act as centers for solidification. Since each grain generated from one single nucleus, as great the number of nuclei, as more grains will form, thus their size will reduce. If the number of nuclei is sufficiently high, dendritic structures could be disappeared as they will have not enough space to grow, and globular grains of primary α-Al will preferentially form.

The SEM photographs of the samples of base alloy in different areas are shown in Figure 5(a, d) as fully dendritic. After the application of cooling rate technique, the morphology of the primary α-Al dendritic crystal was changed into a somewhat globular structure or small polygonal as explained in Figure 4(b, c, e), and the size of the primary α-Al phase reduced obviously from 1400µm to about 50µm. A possible explanation might be the decrease of the intergranular spacing due to the formation of a large number of globular α-Al grains, which might have restricted the growth of the other eutectic silicon, as can be seen in Figure 5(e, f).

The coarse "Chinese script" α-Al_{15}(Fe, Mn)$_3Si_2$ phase was replaced by thin particles with different shapes, with average length value around 50 µm, which is much shorter than non treated A356 alloy, and better distributed throughout the matrix, so this phase was fully refined and homogeneously distributed as small particles throughout the samples.

3.3 The Effect of Cooling Rate on Eutectic Si-Phase

The SEM photographs of the investigated samples are shown in Figure 5. The coarse acicular eutectic silicon is exhibited in the untreated A356 alloy are shown in Figure 5(a, d). At the application of the cooling rate techniques, the size of the eutectic silicon became much smaller and trend to be broken and converted into short sticks or small rounded in other cases as shown in Figure 3(b-f) and Figure 5(e, f). The formation of eutectic silicon usually starts with the formation of Al-rich spikes and consequently the formation of localized eutectic Si enrichment within interdendritic liquid and segregation of numerical small Si needles, as can be used as base particles of β-Al_5FeSi. It is advantageous to the nucleation of eutectic Si and becomes smaller correspondingly than untreated one. In addition, a better distributed throughout the matrix, so this phase was fully refined and homogeneously distributed as small particles throughout the samples. A series of microstructures were quantitatively analysed by using linear intercept method (software). In the base alloy, the average length of eutectic silicon was about 35.2µm, and the average width was 5.0µm with aspect ratio about 7 as shown in Figure 3(a), Table 4 & 5. By cooling, the average length and width become about 9.1µm and 3.4µm, respectively as shown in Fig. 3(b-f), Table 4 & 5, and the aspect ratio became slightly less than 3. Comparing the aspect ratios, the eutectic silicon was significantly refined.

Table 4. Average length of eutectic Si at different mould temperature

Base alloy	25°C	100°C	200°C	300°C	400°C
35.2 µm	9.1 µm	9.9 µm	10.1 µm	10.4µm	10.9µm

Table 5. Average width of eutectic Si at different mould temperature

Base alloy	25°C	100°C	200°C	300°C	400°C
5.0 µm	3.4 µm	3.5 µm	3.7 µm	3.9 µm	4.0 µm

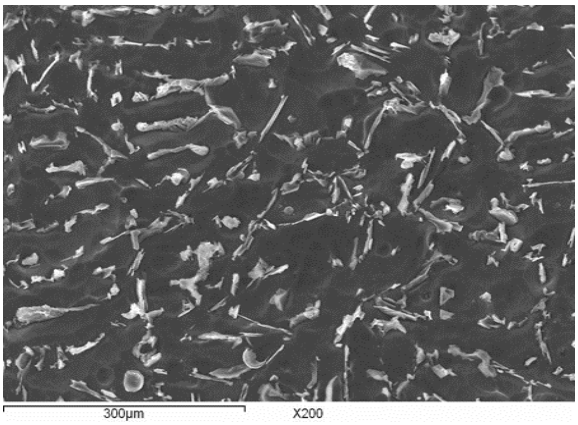

(a) Base alloy

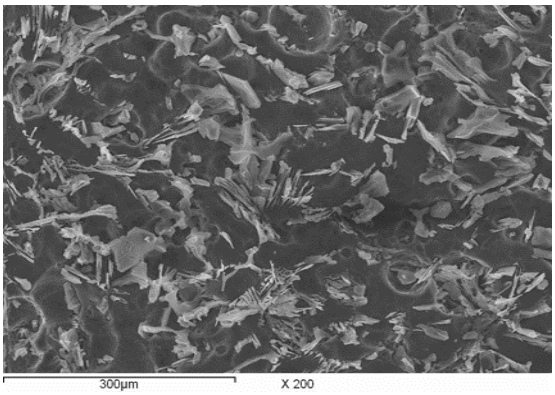

(d) Base alloy

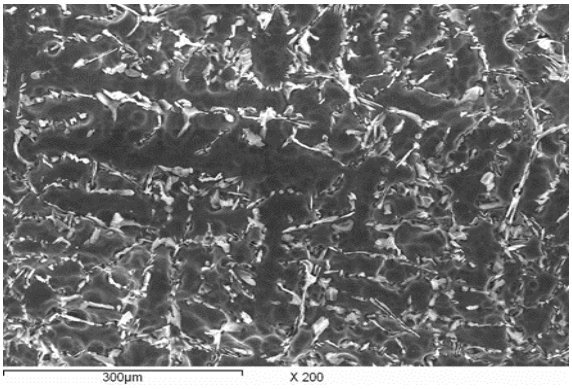

(b) At 25 °C

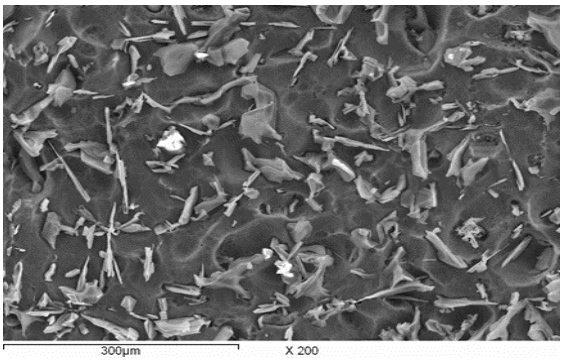

(e) At 25 °C

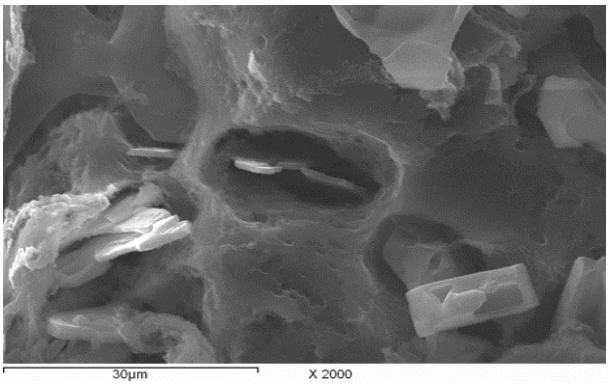

(c) At 25 °C

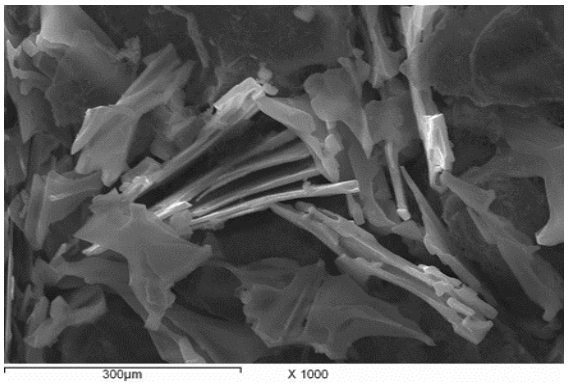

(f) At 25 °C

Figure. 5 SEM photographs of base alloy and silicon structure at cooling rate of 25°C.

Figure 4 showed the three-dimensional SEM morphology of eutectic silicon, the eutectic silicon phase in the base sample exhibited a typical coarse plate-like form, which was also in accordance with previous report [11, 12]. The eutectic structure occurred resulting in a huge reduction of silicon size and changing of eutectic morphology from plate-like structure to thin stick in the samples at cooling rate of 25°C, the silicon morphology is rod-like structure as illustrated in Figure 5(e), and it is trend to be rounded in Figure 3(b-f), then the silicon morphology changed to fibrous form as indicated in Figure 5(f).

4. Conclusions

- Under the solidification conditions that used in this study, it was shown that the increasing of the cooling rate decreases the grain size by increasing the number of substrates that become active nucleants and by decreasing the gradient of the grain size.
- It is clearly refining the microstructure with a larger cooling rate; the dendritic structure of α-phase was broken up and converted into a somewhat globular grain structure.
- At the increasing of cooling rate, the morphology of the eutectic silicon of as-cast A356 alloy could be modified from coarse acicular to short sticks or small rounded in other cases.

Conflict of Interest

"The authors declare no conflict of interest".

5. References

1. Mallapur D.G., Rajendra Udupa k. and Kori S.A.," Influence of Grain Refiner and Modifier On The Microstructure And Mechanical Properties Of A356 Alloy", International Journal of Engineering Science and Technology, Vol. 2(9), 2010, pp.4487-4493.
2. Giulio Timelli, Giordano Camicia and Stefano Ferraro, "Effect of Grain Refinement and Cooling Rate on the Microstructure and Mechanical Properties of Secondary Al-Si-Cu Alloys", Journal of Materials Engineering and Performance, Vol.23(2), Feb. 2014, p.611.
3. Jabbaria M.M., et. al., "Effect of cooling rate on microstructure and mechanical properties of gray cast iron", Materials Science and Engineering: A – Structural Materials: Properties, Microstructure and Processing, Vol.528, Issue 2, 2010, pp. 583-588
4. Liang G., et. al., "Effect of cooling rate on grain refinement of cast aluminum alloys", Materialia, Vol.3, November 2018, pp.113-121.
5. Yang. C.L, et. al., "Effects of cooling rate on solution heat treatment of as-cast A356 alloy", Laboratory of Solidification Processing, Northwestern Polytechnical University, Xi'an 710072, January 2015.
6. Victor. G, et. al., "Correlation between quenching rate, mechanical properties and microstructure in thick sections of Al-Mg-Si(-Cu) alloys". Materials Science & Engineering A, Vol. 753, April 2019, pp. 253-261.
7. Polmear, I.J., "Light Alloys from Traditional Alloys to Nanocrystals", Fourth Edition, Melbourne, Australia, 2006, pp. 205-216.
8. Zhongtao Z., Jie L., Hongyun Y., Jian Z., Tingju L., "Microstructure-. Evolution of 356 Alloy Under Compound Field", Journal of Alloys and Compounds, Vol.484, September 2009, pp. 458–462.
9. John, L., and Bailey, A., ASM Metallographic, Vol. 9, pp. 620-630, 1998.

10. Waly, M.A., Reif. W, "Thermal Analytical Study on the Modification of Al- 7% Si with Addition of Sr&Na", 6th Arab International Aluminum Conference- Arab AL, Cairo 1993.

11. Puga, H., Costa, S., Barbosa, J., Ribeiro, S., and Prokic., M., "Influence of Ultrasonic Melt Treatment on Microstructure and Mechanical Properties of AlSi9Cu3 Alloy ", Journal of Materials Processing Technology, 2011, pp. 1-7.

12. Liu Z.W., Rakita M., Han Q., Li J.G., "Microstructural Evolution Treated by Ultrasonic Vibration", Materials Research Bullet, 2011, pp 1-12.

13. Das, A., and Kotadia., H.R., "Effect of High-Intensity Ultrasonic radiation on the Modification of Solidification Microstructure in a Si-rich Hypoeutectic Al–Si Alloy", Materials Chemistry and Physics, Vol. 125, 2011, pp. 853-859.

14. Jiana X., Meeka T.T., Hanb Q., "Refinement of Eutectic Silicon Phase of Aluminum A356 Alloy Using High-Intensity Ultrasonic Vibration", Script a Materialia, Vol.54, 2006, pp. 893–896.

Citation: Maftah H. Alkathafi, Abdalfattah A. Khalil, Ayad O. Abdalla. “The Effect of Cooling Rate on the Microstructure of A356 Aluminium Alloy”. SVOA Materials Science &Technology, 2020, 2(04): 91-99.